Electronic Journal of Biotechnology 52 (2021) 21–29

Contents lists available at ScienceDirect

Electronic Journal of Biotechnology

journal homepage:

Research Article

Gene expression and apoptosis response in hepatocellular carcinoma cells induced by biocompatible polymer/magnetic nanoparticles containing 5-fluorouracil

Salih Abdul Mahdi [a], Afraa Ali Kadhim [b], Salim Albukhaty [c], Safoora Nikzad [d], Adawiya J. Haider [e], Sumayah Ibraheem [f], Haitham Ali Kadhim [g], Sharafaldin Al-Musawi [a,*]

[a] College of Biotechnology, Al-Qasim Green University, Babylon, Iraq
[b] Department of Biology, College of Science, Mustansiriyah University, Baghdad, Iraq
[c] Department of Chemistry, College of Science, University of Misan, Maysan, Iraq
[d] Department of Medical Physics, Faculty of Medicine, Hamadan University of Medical Sciences, Hamadan, Iran
[e] Applied Science Department/Laser Science and Technology Branch, University of Technology, Baghdad, Iraq
[f] Al_kindy Medicine College, Baghdad, Iraq
[g] Iraq Ministry of Health, Medico Legal Directorate, Baghdad, Iraq

ARTICLE INFO

Article history:
Received 27 October 2020
Accepted 12 April 2021
Available online 1 May 2021

Keywords:
5-Fluorouracil
Apoptosis
Chemotherapeutic drug
Controlled release
Cytotoxicity
Drug delivery
Gene expression
Hepatocellular carcinoma cells
Liver cancer
Magnetic nanoparticles
Super-paramagnetic iron oxide nanoparticles
Targeted delivery

ABSTRACT

Background: Super-paramagnetic iron oxide nanoparticles (SPION) contain a chemotherapeutic drug and are regarded as a promising technique for improving targeted delivery into cancer cells.
Results: In this study, the fabrication of 5-fluorouracil (5-FU) was investigated with loaded Dextran (DEX-SPION) using the co-precipitation technique and conjugated by folate (FA). These nanoparticles (NPs) were employed as carriers and anticancer compounds against liver cancer cells in vitro. Structural, magnetic, morphological characterization, size, and drug loading activities of the obtained FA-DEX-5-FU-SPION NPs were checked using FTIR, VSM, FESEM, TEM, DLS, and zeta potential techniques. The cellular toxicity effect of FA-DEX-5-FU-SPION NPs was evaluated using the MTT test on liver cancer (SNU-423) and healthy cells (LO2). Furthermore, the apoptosis measurement and the expression levels of NF-1, Her-2/neu, c-Raf-1, and Wnt-1 genes were evaluated post-treatment using flow cytometry and RT-PCR, respectively. The obtained NPs were spherical with a suitable dispersity without noticeable aggregation. The size of the NPs, polydispersity, and zeta were 74 ± 13 nm, 0.080 and −45 mV, respectively. The results of the encapsulation efficiency of the nano-compound showed highly colloidal stability and proper drug maintenance. The results indicated that FA-DEX-5-FU-SPION demonstrated a sustained release profile of 5-FU in both phosphate and citrate buffer solutions separately, with higher cytotoxicity against SNU-423 cells than against other cells types. These findings suggest that FA-DEX-SPION NPs exert synergistic effects for targeting intracellular delivery of 5-FU, apoptosis induction, and gene expression stimulation.
Conclusions: The findings proved that FA-DEX-5-FU-SPION presented remarkable antitumor properties; no adverse subsequences were revealed against normal cells.
How to cite: Mahdia SA, Kadhimb AA, Albukhaty S, et al. Gene expression and apoptosis response in hepatocellular carcinoma cells induced by biocompatible polymer/magnetic nanoparticles containing 5-fluorouracil. Electron J Biotechnol 2021;52. https://doi.org/10.1016/j.ejbt.2021.04.001

1. Introduction

Among the chemotherapeutic agents, 5-Fluorouracil (5-FU) is frequently used to treat liver cancer, in addition to its diverse types of malignancies, such as colon and pancreatic cancer [1]. It is characterized by cellular toxicity, its work on interference, and its inhibition of DNA synthesis, which terminates cell growth [2]. The agent 5-FU is regarded as one of the most common anticancer drugs associated with broadside effects, such as hematological disturbances, the toxicity of the gastrointestinal tract, and bone marrow deficiency, which makes it limited for clinical usage [3,4]. Nano-drug delivery systems with a nanobiotechnological base

Peer review under responsibility of Pontificia Universidad Católica de Valparaíso
* Corresponding author.
E-mail address: dr.sharaf@biotech.uoqasim.edu.iq (S. Al-Musawi).

https://doi.org/10.1016/j.ejbt.2021.04.001
0717-3458/

could be developed by improving the biocompatible nanoparticles. It represents a significant example of releasing the drug directly to the targeted cancer-affected location using a low concentration and toxicity. Tests have shown promising alternative approaches for drug delivery instead of the classical methods [5,6]. SPIONs have broad potential for cancer detection and treatment. These nanoparticles have been used in magnetic resonance imaging (MRI) as contrast agents and nanocarriers for therapeutic gene and drug delivery vehicles [7,8,9]. These systems allow the extensive delivery of a local drug, which provides an increase in medicine concentrations inside the cancer cells, such as the medium and minimum concentrations of the drug in the bloodstream and other tissues [10]. In modern research, the targeting delivery of chemotherapy factors in cancer cells by super-paramagnetic iron oxide nanoparticles has been investigated and studied by many researchers and has provided useful and desirable results [11]. Drug delivery approaches provide an enhancement of treatment due to the alteration of drug properties [12], which leads to an increase in the bioavailability of the medicines in the bloodstream and a decrease in the toxicity, as well as an increase in the half-life of medication [13]. These characteristics were accomplished by improving drug delivery via SPIONs with its unique features as a drug carrier [14]. The encapsulation of SPIONs with polysaccharides, such as dextran, increases biocompatibility and mitigates the toxicity of SPIONs [15]. The reactive oxygen species (ROS) relies on the stability of the encapsulating factor, its tendency for producing ROS, and concentrates on the cells [16]. FA is overexpressed on the surfaces of different kinds of cancer, including liver cancer cells; therefore, it has been employed to target the therapeutic agents of cancer [17]. According to those mentioned earlier, the present study has been achieved using an active carrier framework design by a synthesis of dual targeting SPION-DEX-FA (Fig. 1). This is an excellent scale with biocompatible properties that are tumor-specific, and it incorporates those for liver cancer cells. Additionally, the gene expression levels were extended by corroborating selected results of the RT-PCR analysis.

2. Materials and methods

2.1. Materials

The following were purchased from Merck (Darmstadt, Germany): 5-FU, dextran (15 kDa), ferric chloride hexahydrate dimethyl sulfoxide (DMSO), ($FeCl_3{\cdot}6H_2O$), ferrous chloride tetrahydrate ($FeCl_2{\cdot}4H_2O$), MTT agent and NH4OH (25% ammonia), DEX and FA. Annexin V\FITC, propidium iodide (PI), trypan blue, 96-well cell culture plates, and flasks were purchased from Sigma-Aldrich (St. Louis, MO, USA). SNU-423 and the Lo2 cell line were obtained from the Pasteur Institute of Iran.

2.2. Fabrication of DEX-SPION

The SPION was fabricated using the co-precipitation method [18]. N2 gas was poured into 55 mL of distilled water. Then, 2 mmol of FeCl2·4H2O, 4 mmol of FeCl3·6H2O, and 10 mL of 0.5% dextran were placed into the solution. Following that, NH4OH was added dropwise using a syringe. Subsequently, the mixtures were stirred at 65 °C for 30 min under a nitrogen atmosphere and centrifuge, and the formed black precipitates were collected.

2.3. Preparation of FA-DEX-5-FU-SPION

Briefly, 100 mg of a prepared DEX-SPION was added to 20 mg 5-FU (previously dissolved in 20 mL of DMSO) and stirred for 24 h. Afterward, FA functionalization of this nano-formulation was performed by adding 5 mg/ml of this molecule to the obtained mixture (FA-DEX-5-FU-SPION). The surface functionalization of DEX-5-FU-SPION was conducted due to the electrostatic reactions. The FA-DEX-5-FU-SPION was detached by centrifugation at 15000 rpm and then re-washed three times with distilled water. A vacuum oven was used to dry the 5-FU entrapped nanoparticles at 40 °C for 8 h. The unloaded 5-FU was calculated by measuring its concentration in the supernatant. The efficacy of drug encapsulation was calculated using the following Equation (1) [9]:

$$\textit{Encapsulation efficiency}(\%) = \frac{(\textbf{Whole quantity of drug} - \textbf{free quantity of drug})}{\textbf{Overall amount of drug}} \times 100 \quad (1)$$

2.4. Size and morphological characterization of NPs

The size and morphological features of the obtained FA-DEX-5-FU-SPION nanocomposite were estimated using high-resolution transmission electron microscopy (TEM) and scanning electron microscopy (SEM) experiments (Hitachi High-Technologies Corporation, Tokyo, Japan) at 30.0 kV voltage and 30 mA. The zeta potential and DLS (MALVERN, Nano S, United Kingdom) were performed. Fourier transform infrared (FTIR) spectra were recorded on a Thermo Nicolet 6700 (AEM, Madison WI, USA) within a range of 400 cm^{-1}–4000 cm^{-1}. Additionally, a vibrating sample magnetometer (VSM, Lakeshore 7404, USA) was performed to evaluate the magnetic properties.

2.5. Measurement of drug release

The 5-FU drug release from FA-DEX-SPION was performed in phosphate (PBS) (0.01 M with pH 7.4) and citrate (0.01 M with pH 5.4) buffers at 37 °C. One ml of the drug-loaded micellar solution was poured into two separate dialysis bags (Spectra/por, MW cut off 3500 gmol-1). These bags were placed into phosphate (100 ml, 0.01 M, pH 7.4) and citrate (100 ml, 0.01 M, pH 5.4) buffers separately. Tween 80, as the emulsifier agent, was added to each of these buffer solutions to inhibit the possible sedimentation of the released drug. The temperature was fixed at 37 °C, and the buffer was agitated gently by a shaker (GFL, Burgwedel, Germany). Sampling was performed at zero, four, eight, 12, 24, 48, 72, and 96 h at fixed time intervals. At each time point, 500 µl of the

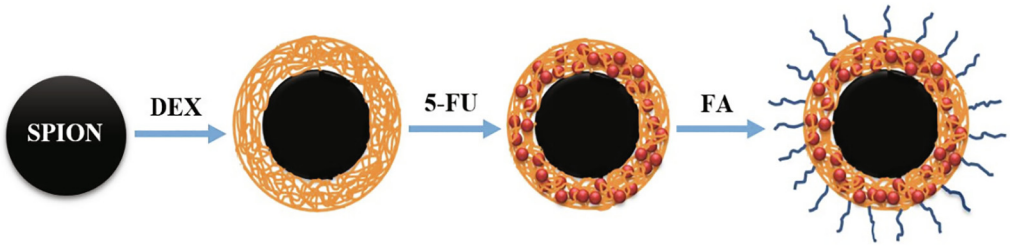

Fig. 1. Schematic illustration of the procedure for synthesis and formulating FA-DEX-5-FU-SPION nanoparticles.

specimen was collected and subjected to freeze-drying. The residue was dissolved in 2 ml of methanol. The quantity of the released 5-FU was determined using a nanodrop [19]. Drug release was measured using the following:

$$R = \frac{V\sum_{i}^{n-1} C_i + V_o C_n}{m_{drug}} \quad (2)$$

where R is the drug release accumulation (%), V is the sampling volume, V_0 is the first volume of the drug, C_i and C_n are the 5-FU concentrations, i and n are the sampling times and m_{drug} is the mass of the loaded 5-FU in FA-DEX-SPION. The precipitated material was rinsed and suspended again with DDW.

2.6. Cell culture condition

Liver cancer cells (SNU-423) were incubated in the culture media (DMEM), supplemented with 10% fetal bovine serum (FBS) and penicillin/streptomycin (Gibco, Life Technologies, Paisley, United Kingdom), and grown in a humidified incubator of 5% CO2 at 37 °C (Plymouth, MN, United States of America).

2.7. Cell internalisation assay

FA-DEX-5-FU-SPION was functionalized using FITC (Fluorescein 5(6)- Isothiocyanate) to evaluate its cell internalization efficiency by a fluorescence microscope (Nikon Eclipse TE2000-U). Therefore, the cells were treated with 5 μg FITC-FA-DEX-5-FU-SPION for three hours. Subsequently, the nanocomposite-included media were thrown out, and the cells were washed with phosphate-buffered saline (PBS). Cell photography was carried out using a fluorescence microscope (Nikon Eclipse TE2000-U). To study the efficiency of FA-DEX-SPION in activating the bioavailability of 5-FU, fluorescence microscopy was used to examine the cells [20].

2.8. MTT assay

To fulfill the MTT, a 200 μl medium containing 1×10^4 cells was poured into each well of a 96 well cell plate. The cells were adhered to and grown for 24 h. The medium of each well was removed and replaced with a fresh one containing various concentrations (4 μg to 20 μg) of either 5-FU, FA-DEX-5-FU-SPION, or FA-DEX-SPION. The incubation periods of 24 and 48 h were considered. A group of cells without treatment was regarded as the control. A suitable concentration of the MTT solution (10 μl of the 5 mg/ml solution in each 100 μl media) was added to each well. The plates were incubated at 37 °C in a humidified atmosphere containing 95% air and 5% CO2 for four hours. The remaining MTT solution was removed, and 100 μl of DMSO was added to each well to dissolve the formazan crystals. The plates were shaken for five minutes to ensure the adequate dissolution of the formazan crystals. The absorbance of each well was recorded at 540 nm using a multi-scan plate reader (VERSAmax microplate reader, Molecular Device, CA, USA). The results were obtained using mean ± SD.

$$Relative\ cell\ toxicity = \left[\frac{A_{\text{sample}} - A_{control}}{A_{control}}\right] \times 100 \quad (3)$$

Table 2
Temperature, time, and the number of cycles for each step.

Step	Temperature	Time	Cycles
Initial Denaturation	95 °C	10 min	1
Denaturation	95 °C	15 s	48
Annealing	60 °C	1 min	
Melting curve analysis	95 °C	5 s/step	1

2.9. Apoptosis assay by flow cytometry

The flow cytometry assay was applied to estimate the average of apoptosis and necrosis in cells exposed to different treatments of nano-drug composite, void 5-FU, and FA-DEX-5-FU-SPION for 48 hours and was stained using Annexin V–FITC and propidium iodide (PI). After that, the cells were harvested using trypsin, counted, and then poured into six-well plates for around 10^4 cells / well. Apoptosis was estimated using the Annexin V-FITC Apoptosis Detection Kit (Biovision, Inc.) depending on the manufacturer's protocols.

2.10. RT-PCr

2.10.1. Isolation of total RNA and complementary DNA synthesis

After 48 h of SNU-423 cell treatment, the total RNA was extracted from the cell lysates using TRIzol (Invitrogen Life Technologies, United Kingdom). The concentrations and quantities of the RNA were quantified by measuring the optical density OD (260/280 wavelength). The total RNA is classically used in the cDNA synthesis kit (Fermentas, Germany). According to the manufacturer's instructions for the kit, five pairs of oligonucleotide primers for targets and endogenous genes were used, as illustrated in Table 1.

2.10.2. Quantitative real-time PCR reaction

To estimate the expression levels of the NF-1, Her-2/neu, c-Raf-1, and Wnt-1 genes, real-time PCR was achieved on the ABI prism (Applied Biosystems, USA). Beta-actin was the reference control gene. The amplification reactions contained 5 μL of cDNA, 10 μL of the SYBR Green-I dye (Applied Biosystems, USA), and 0.5 μL of each specific primer. PCR was carried out for 50 cycles initiated at 95 °C for ten minutes, 95 °C for 15 s, and 60 °C for 1 min, and the Real-Time PCR success was examined using the melting curve analysis (Table 2).

3. Result and discussion

3.1. Characterisation of synthesized nanoparticles

The FA-DEX-5-FU-SPION synthesis nanoparticles were comprehensively examined using DLS (Fig. 2A). Fig. 2A shows the size of FA-DEX-5-FU-SPION, and its polydispersity at 25 °C was 74 ± 13 nm and 0.080 nm, respectively. Fig. 2B shows the zeta potential results with a negative surface charge in 5-FU-loaded DEX-SPIONs. Furthermore, the high-resolution transmission electron microscope (TEM) and field emission scanning electron microscope (SEM) were applied to recognize the synthesis

Table 1
Primers were used for β-Actin, NF1, Her-2 / neu, c-Raf-1, and Wnt-1 genes in the present study.

Primer Name	Primer sequenceOligo sequence F (5′ 3′)	Primer sequenceOligo sequence R (5′ 3′)	References
β-actin	CATGTACGTTGCTATCCAGGC	CTCCTTAATGTCACGCACGAT	[42]
NF-1	GGGCAGTATCTTTCCAGCAACAG	GTTAAGGCTGGACCAGTGTG	[43]
Her-2/neu	ACCTGCTGAACTGGTGTATGCA	GTGTACGAGCCGCACATCCT	[44]
c-Raf-1	GAACTGCCCCAAAGCAATGA	CACCTTTTTCACACAGTCGGC	[45]
Wnt-1	ATGAACCTTCACAACAACGAG	GGTTGCTGCCTCGGTTG	[46]

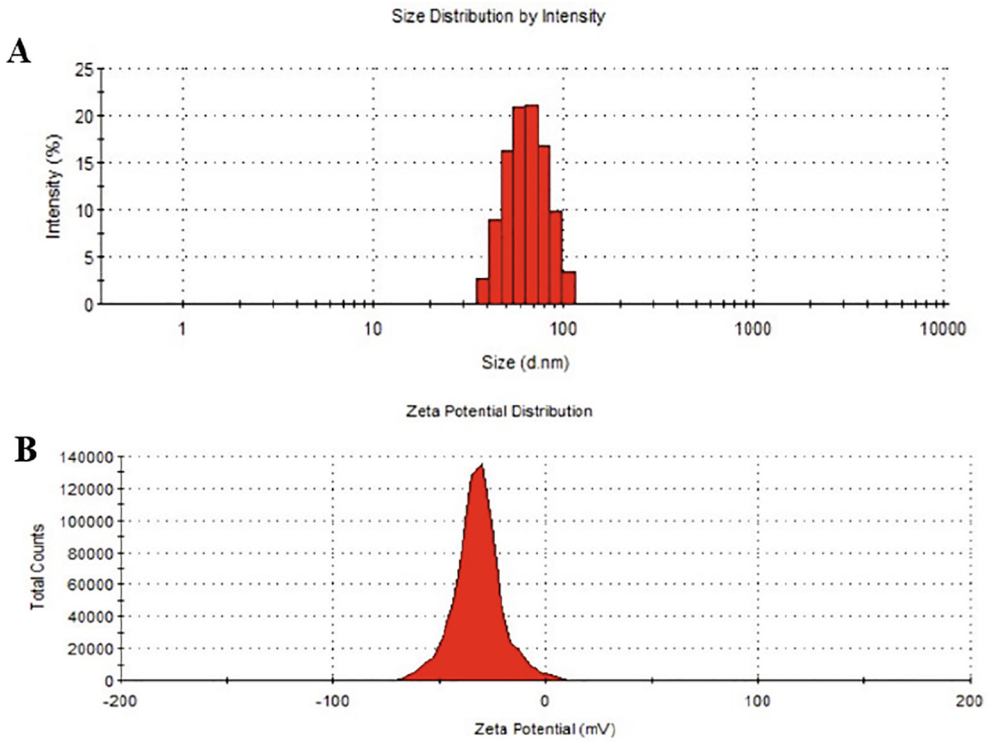

Fig. 2. Nano-formulation size (A) and charge (B) images. The FA-DEX-5-FU-SPION charge using dynamic light scattering (DLS).

nanoparticles' structural order, size, and shape. The result of the synthesized nanoparticles exhibited that the NPs were smooth, ball-shaped, and had no adhesion between them (Fig. 3A, B). It is observed that the particles were obtained in this study uniform in size and spherical.

Fourier-transform infrared spectroscopy (FTIR) spectra for 5-FU and DEX-SPIONs-FA, as shown in Fig. 4A and B, exhibited the spectrum of 5-FU at approximately 1500 cm^{-1}, as well as intense broadband at 1280 cm^{-1}. The magnetic properties of NPs were described using vibrating sample magnetometry (VSM). The NPs produced a magnetization curve with zero remanences and coercivity. According to Fig. 4B, the saturation magnetization was 57 emu/g, which is a positive result compared to the typical values of 30–50 emu/g that were recorded in the literature for SPIONs that were obtained by co-precipitation [15].

3.2. The encapsulation efficiency of FA-DEX-5-FU-SPION

The encapsulation of 5-FU in DEX-SPION-FA was studied using Equation (1). The calculation for the encapsulation efficiency was 83.2 ± 3.4, which means a proper loading of drugs on DEX-SPION was achieved.

3.3. Release profile

Based on the result of the in vitro release curves, as shown in Fig. 5, the 5-FU release time from the loaded FA-DEX-5-FU-SPION nanosystem over 96 h was faster in the citrate buffer with an acidic pH of 5.4 compared to the phosphate buffer with a normal pH 7.4 and pH 5.4 under the same conditions.

3.4. Cellular internalization

5-FU loaded FA-DEX-SPION nanoformulation was effectively internalized within the cancer cells and was visualized by fluorescence microscopy (Fig. 6B, C), while void 5-FU was aggregated as crystal bodies of various sizes (Fig. 6A). SNU-423 cells treated with FA-DEX-5-FU-SPION seemed green because of the significant uptake volume due to the enhanced 5-FU solubility after loading onto the FA-DEX-SPION nanocarrier. In comparison, green,

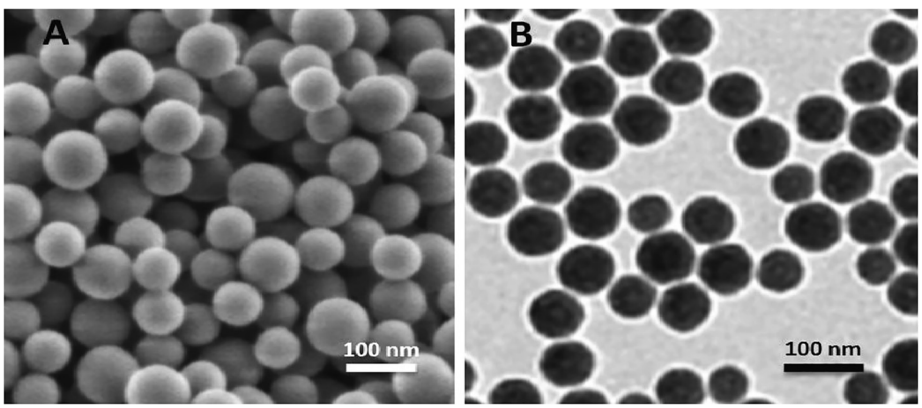

Fig. 3. Microscopic analysis of FA-DEX-5-FU-SPION (A) SEM image of FA-DEX-5-FU-SPION (B) TEM image of FA-DEX-5-FU-SPION.

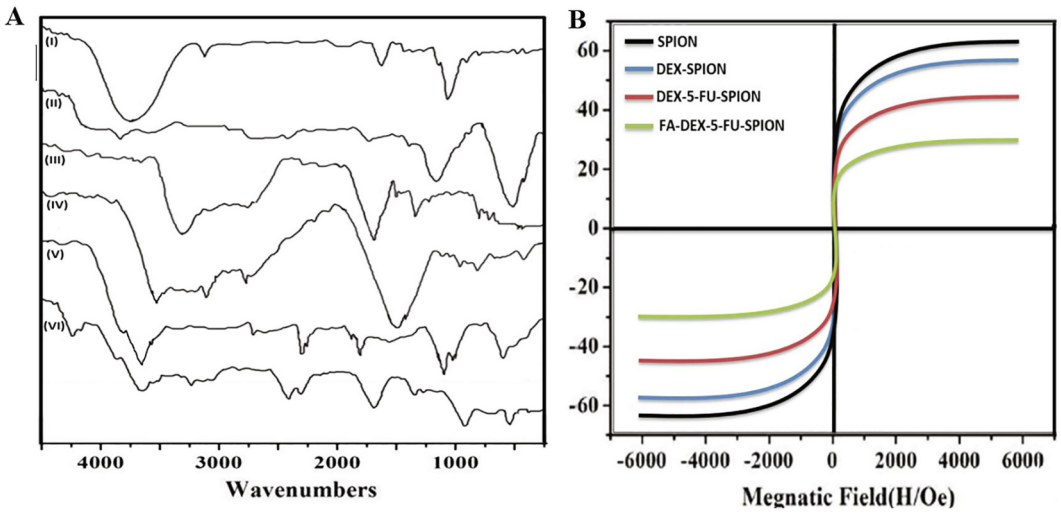

Fig. 4. FT-IR spectra of DEX (I), SPION (II), 5-FU (III), FA (IV), DEX-SPION (V) and FA-DEX-5-FU-SPION (VI). (A) The magnetization curve loop of SPION, DEX-SPION, DEX-5-FU-SPION, and FA-DEX-5-FU-SPION at 300 K (B).

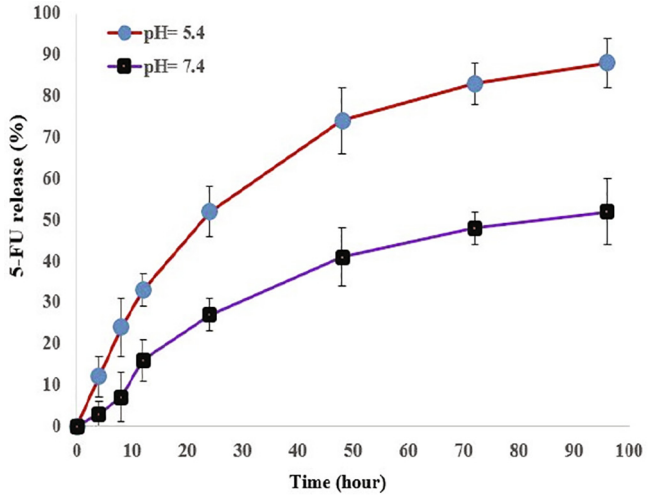

Fig. 5. In vitro release profile of FA-DEX-5-FU-SPION nano-formulation at pH 7.4 and pH 5.4. All experiments were performed at 37 °C. The data represent the mean values ± SD (n = 3).

star-like, and insoluble particles were visible in the intercellular space in cells treated with void 5-FU because of their insolubility in an aqueous medium.

3.5. Cytotoxicity assay

The cellular toxicity of non-conjugated 5-FU was initially determined, along with the bare nanoparticle FA-DEX-SPION and nanocomposite FA-DEX-5-FU-SPION, using MTT on SNU-423 cancer and LO2 healthy cells. The curve, as shown in Fig. 7, signifies the test that was achieved in two time periods of 24 and 48 h. Moreover, all the cells were treated with different concentrations (4 μg–20 μg). The results show that the nano-formulated FA-DEX-5-FU-SPION significantly inhibited the proliferation of SNU-423 cancer cells in comparison with bare FA-DEX-SPION and void 5-FU. However, no significant differences were observed in the proliferation of healthy LO2 cells for the FA-DEX-5-FU-SPION treatment. The studied IC50 results showed 15.28 μg and 10.54 μg concentrations for 24 and 48 h, respectively. Additionally, both the bare FA-DEX-SPION and void 5-FU treatments did not show any significant cytotoxicity in all the used concentrations. Based on the present results, FA-targeted DEX and SPION NPs were more powerful in improving the effectiveness and efficiency of 5-FU. Activity, dose, and treatment period for 5-FU, FA-DEX-5-FU-SPION, and FA-DEX-SPION were selected after an assessment of different doses and concentrations in cytotoxicity study and reach to best doses treatments in cancer cells [21,22].

3.6. Apoptosis measurement by flow cytometry

Regarding estimating the cytotoxic effect of FA-DEX-5-FU-SPION on SNU-423 cells, flow cytometry was achieved 48 h after

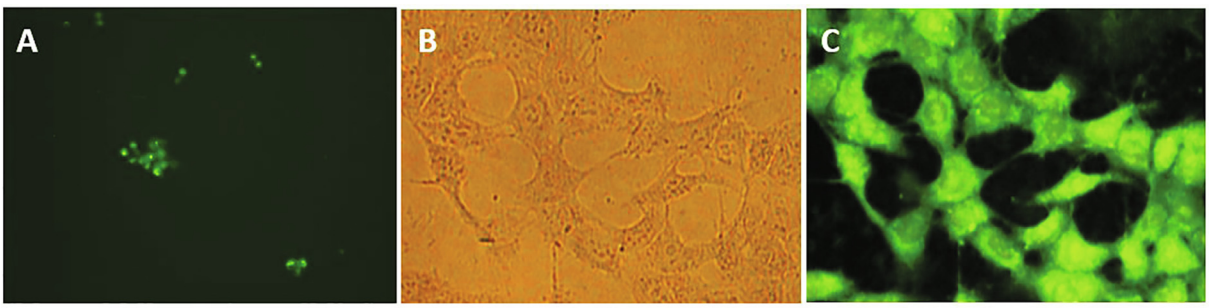

Fig. 6. Cell internalization study of FA-DEX-5-FU-SPION in the SNU-423 cancer cells using fluorescence microscopy (400× magnification). Fluorescence microscopy image of 5-FU-treated cells (A). Optic microscopy image of FA-DEX-5-FU-SPION-treated cells (B). Fluorescence microscopy image of FA-DEX-5-FU-SPION-treated cells (C).

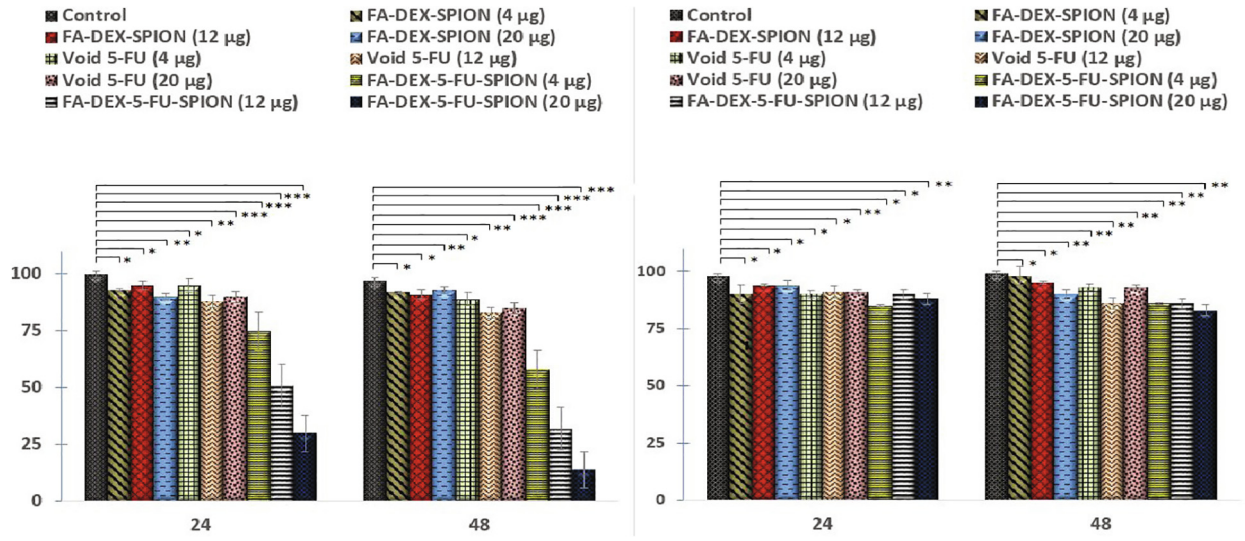

Fig. 7. MTT assay for the FA-DEX-5-FU-SPION nano-formulation, void 5-FU, and FA-DEX-SPION at 24 h and 48 h on SNU-423 (A) and Lo2 cell lines (B).

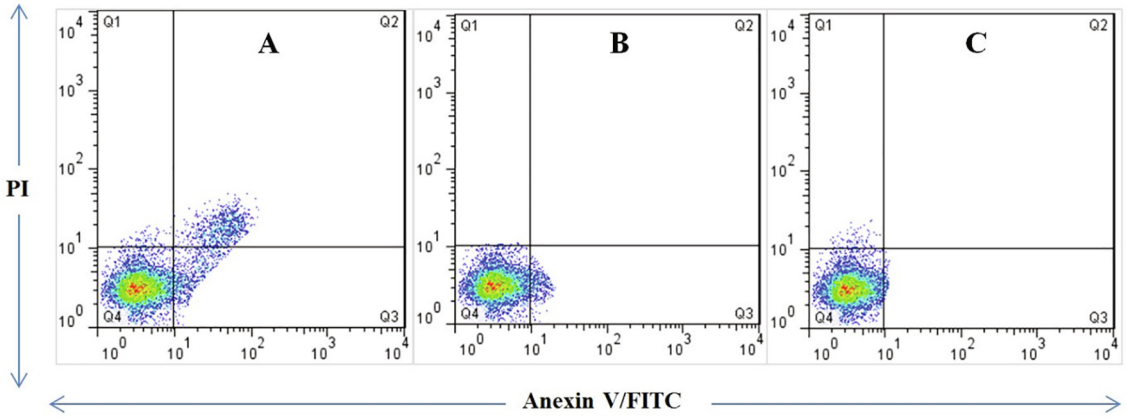

Fig. 8. Apoptosis induction by FA-DEX-5-FU-SPION nano-formulation. The SNU-423 cell line was treated with (A) FA-DEX-5-FU-SPION (B) bare FA-DEX-SPION and (C) void 5-FU. The number of SNU-423 cells undergoing apoptosis increases when treated with FA-DEX-5-FU-SPION nano-formulation. Moreover, treatment of the SNU-423 cell line with bare FA-DEX-SPION and void 5-FU separately indicates that both treatments did not show any remarkable apoptosis induction.

treatment. The results in Fig. 8 illustrate a significant enhancement that was carried out as a percentage of the apoptotic cells in the case of the cancer cell line. As realized in this figure, the FA-DEX-5-FU-SPION nanoformulation revealed noticeable apoptosis in cancer cells, whereas there was no significant apoptotic effect achieved using the same concentration of FA-DEX-SPION.

3.7. Gene expression

To understand the pathway(s) that mediated the apoptosis induced by FA-DEX-5-FU-SPION, we examined the rates of expression of the genes NF-1, Her-2/neu, c-Raf-1, and Wnt-1. As mentioned above, the expression levels of the NF-1, Her-2/neu, c-Raf-1, and Wnt-1 genes were studied with qPCR, and beta-actin was used as the reference control gene (housekeeping gene). All candidate genes had significantly different expressions between malignant and non-malignant samples, as shown in Fig. 9. The expression levels of beta-actin remained constant among the control and cancerous cells with and without treatment with 5-FU. However, the expression level of the NF-1 gene delivered a significantly high rate in the cancerous

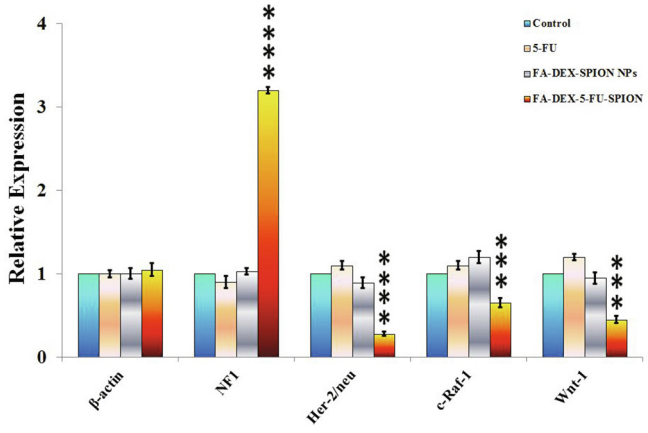

Fig. 9. Real-time PCR gene expression analysis of SNU-423 cell lines treatments with void 5-FU, FA-DEX-5-FU-SPION, and FA-DEX-SPION by two-way ANOVA and Bonferroni post-test. Values in the graph represent mean ± SD. $^{**}P < 0.01$, $^{***}P < 0.001$ and $^{****}P < 0.0001$ indicate significant differences between the control (untreated) and other treatments.

cells when it was treated with FA-DEX-5-FU-SPION compared to void 5-FU and FA-DEX-SPION (****$P < 0.0001$) (Fig. 9).

4. Discussion

In the current study, a nanoscale composite, which was made from DEX-SPION-FA carrying the 5-FU drug, was prepared to compare the cytotoxic effects post-treatment (free or loaded into DEX-SPION-FA nanoparticles) on liver cancer cells (SNU-423 cancer and LO2 healthy cell lines) in vitro. The size of the nanoparticles is an essential part of the drug delivery process. The tumor cells ranged from 100 nm to 780 nm in size [21]. FA-DEX-5-FU-SPION nanoparticles that were obtained in this study were 74 ± 13 nm in size, which was smaller than those that were used in the formerly reported study [9]. Then, these NPs were permitted to enter the spaces inside the tumor cells. Eynali et al. [23] studied 5-FU encapsulation efficiency using PLGA nanoparticles coated with magnetic iron oxide NPs at 71.8%. Higher loading could be attributed to the type of core–shell structure, and the presence of polymer provides several functional groups for more significant interaction with drug molecules on the drug delivery system's surface [24]. The nanocomposite exhibited high stability and appropriate drug conservation at this time. Moreover, Al-Musawi et al. [9] achieved the same result regarding the 5-FU release profile using magnetic iron oxide NPs coated with chitosan. Eynali et al. [23] roved similar cumulative in vitro release profiles of 5-FU from the polymeric-coated iron oxide core with pH 7.4 at different temperatures. This result clearly shows that FA-DEX-5FU-SPION is a potent carrier that can be used as a delivery mechanism for targeted drugs for cancer. The cytotoxicity results show that the nano-formulated FA-DEX-5-FU-SPION significantly inhibited the proliferation of SNU-423 cancer cells in comparison with bare FA-DEX-SPION and void 5-FU. However, no significant differences were observed in the proliferation of healthy LO2 cells for FA-DEX-5-FU-SPION treatment. The studied IC50 results showed 15.28 μg and 10.54 μg concentrations for 24 and 48 h, respectively. Additionally, both the bare FA-DEX-SPION and void 5-FU treatments did not show any significant cytotoxicity in all the used concentrations. A study by Ebadi et al. [21] reported that for the IC50 of 5-FU loaded polyethylene glycol-coated magnetic layered double hydroxide (PEG-FU-MLDH) against liver cancer cells, HepG2 was found to be 28.88 μg/mL. Eynali et al. [23] showed that PLGA nanoparticles as 5-FU carriers significantly enhanced the cytotoxic effects in cancer cells as compared to the control group. Furthermore, Albukhaty et al. [25] using the same nanocarrier in cancer cell treatment. Their result showed that and reported that FA-DEX-SPION possesses noticeable biocompatibility as well as remarkable drug targeting properties. Additionally, their findings proved that drug-loaded FA-DEX-SPION has significant toxic efficacy against treated cancer cell lines. Al-Musawi et al. [9] used the same 5-Fu nanocarrier with chitosan polymer in their applied nanocarrier instead of DEX polymer for bladder cancer therapy. Their data show a similar anti-cancer effect of 5-Fu nanocarrier against cancer cells. Based on the present results, FA-targeted DEX and SPION NPs were more powerful in improving the effectiveness and efficiency of 5-FU. Folate is considered important for the absorption of cancer cells over-expressed by the folate receptors. Folate receptors are over-expressed on the surface of different cancer cells, while little is expressed on the surface of normal cells. Furthermore, from the obtained results, it is apparent that the folate-dextran nanoformulation has significant cytotoxic activity against cancer compared with other nanocarrier formulations. It aids in the sustained release of the drug for the treatment of cancer [26,27,28]. Over recent years, it has become clear that many anti-cancer drugs trigger apoptosis and necrosis in cancer cells by activating reactive oxygen species (ROS) production [29,30,31]. The data indicated that FA-DEX-5-FU-SPION NPs revealed better anticancer activity, as shown through cell apoptosis, induced attenuation of cellular proliferation and tumor growth. The anti-tumor activity by 5-FU is caused by inhibiting cell cycle progression to stimulating DNA damage, which results in cellular apoptosis [32]. NF-1 acts as a tumor suppressor protein [33,34]. The results showed that NF1 is highly expressed in the treated SNU-423 cells with 5-FU-loaded DEX-SPION-FA nanoparticles, as shown by qRT-PCR. Successful targeting was delivered to the site of action by interacting with its receptor on the cell, which is indicated its inhibition effect on cellular tumor growth and proliferation. On the other hand, Her-2/neu, c-Raf-1, and Wnt-1 played an essential causal role in carcinogenesis, and their low expression in cells showed a reliable indicator for treatment response [35,36,37,38,39,40,41]. It was found that the indicated low expression levels of *Wnt-1, c-RaF-1,* and *Her-2/neu* genes were visibly reduced in cancerous cells when treated with FA-DEX-5-FU-SPION compared with void 5-FU and FA-DEX-SPION. This indicates that the drug was successfully delivered to the site of action of the cancerous cells. Because of the novelty of this work, so far, there have been no data about the 5-FU up and down regulating effects in the NF-1, Her-2/neu, c-Raf-1, and Wnt-1 genes expression for different cancers.

5. Conclusion

Super-paramagnetic nanoparticles coated with dextran (DEX-SPION) and carrying 5-fluorouracil were successfully fabricated using the co-precipitation approach. The nano vehicle improved the drug loading with nanoscale particle size distribution. The results indicate that FA-DEX-5-FU-SPION is a consistent co-delivery system for 5-FU. FA-DEX-5-FU-SPION nanoparticles have a sustainable release profile, which leads to dose- and time-dependent targeted liver cell cytotoxicity. FA-DEX-5-FU-SPION has an inhibiting activity against tumor growth in liver cancer, which is more marked than 5-FU and FA-DEX-SPION by themselves. Moreover, FA-DEX-5-FU-SPION has high biocompatibility, loading efficiency, controllability, and penetrability, which made it a useful and exciting tool for a wide range of potential applications in biomedicine. It is recommended that FA-DEX-5-FU-SPION could induce cytotoxic effects on Wnt-1, c-RaF-1, and Her-2/neu gene expression levels, as well as a reduction in cancerous cells. It could thereby effectively control the progression without toxicity to healthy cells compared to void 5-FU and FA-DEX-SPION. Therefore, it could be applied as a safe and active anti-tumor factor for use in clinical settings.

Acknowledgments

The authors extend their appreciation to Al-Qasim Green University and the University of Misasacknn for their technical support.

Conflicts of interest

The authors declare no conflict of interest.

References

[1] Kusano M, Aoyama T, Okabayashi K, et al. A randomized phase III study of hepatic arterial infusion chemotherapy with 5-fluorouracil and subsequent systemic chemotherapy versus systemic chemotherapy alone for colorectal cancer patients with curatively resected liver metastases (Japanese Foundation for Multidisciplinary Treatment of Cancer 32). J Cancer Res Ther 2018;14 (10):761. https://doi.org/10.4103/0973-1482.179188. PMid: 30249900.

[2] Cheng M, He B, Wan T, et al. 5-Fluorouracil nanoparticles inhibit hepatocellular carcinoma via activation of the p53 pathway in the orthotopic transplant mouse model. PLoS ONE 2012;7(10):e47115. https://doi.org/10.1371/journal.pone.0047115. PMid: 23077553.
[3] He YC, Chen JW, Cao J, et al. Toxicities and therapeutic effect of 5-fluorouracil controlled release implant on tumor-bearing rats. World J Gastroenterol 2003;9(8):1795–8. https://doi.org/10.3748/wjg.v9.i8.1795 PMid: 12918123.
[4] Fidai SS, Sharma AE, Johnson DN, et al. Dihydropyrimidine dehydrogenase deficiency as a cause of fatal 5-Fluorouracil toxicity. Autops Case Rep 2018;8 (4):. https://doi.org/10.4322/acr.2018.049. PMid: 30775324e2018049.
[5] Al-Kinani MA, Haider AJ, Al-Musawi S. Design, construction and characterization of intelligence polymer coated core-shell nanocarrier for curcumin drug encapsulation and delivery in lung cancer therapy purposes. J Inorg Organomet Polym 2021;31(1):70–9. https://doi.org/10.1007/s10904-020-01672-w.
[6] Azandaryani AH, Kashanian S, Jamshidnejad-Tosaramandani T. Recent insights into effective nanomaterials and biomacromolecules conjugation in advanced drug targeting. Curr Pharm Biotechnol 2019;20(7):526–41. https://doi.org/10.2174/1389201020666190417125101 PMid: 31038063.
[7] Moradi Khaniabadi P, Shahbazi-Gahrouei D, Jaafar MS, et al. Magnetic iron oxide nanoparticles as T2 MR imaging contrast agent for detection of breast cancer (MCF-7) cell. Avicenna J Med Biotechnol 2017;9(4):181–8. PMid: 29090067.
[8] Albukhaty S, Naderi-Manesh H, Tiraihi T, et al. Poly-L-lysine-coated superparamagnetic nanoparticles: a novel method for the transfection of pro-BDNF into neural stem cells. Artif Cells Nanomed Biotechnol 2018;46(3): S125–32. https://doi.org/10.1080/21691401.2018.1489272 PMid: 30033772.
[9] Al-Musawi S, Hadi AJ, Hadi SJ, et al. Preparation and characterization of folated chitosan-magnetic nanocarrier for 5-fluorouracil drug delivery and studying its effect in bladder cancer therapy. J Glob Pharm Technol 2019;11:628–37.
[10] Al-Musawi S, Kadhim MJ, Hindi NKK, et al. Folated-nanocarrier for paclitaxel drug delivery in leukemia cancer therapy. J Pharm Sci Res 2018;10(4):749–54.
[11] Elsherbini A, Bieberich E. Ceramide and exosomes: a novel target in cancer biology and therapy. Adv Cancer Res 2018;140:121–54. https://doi.org/10.1016/bs.acr.2018.05.004 PMid: 30060807.
[12] Al-Awady MJ, Balakit AA, Al-Musawi S, et al. Investigation of anti-MRSA and anticancer activity of eco-friendly synthesized silver nanoparticles from palm dates extract. Nano Biomed Eng 2019;11. https://doi.org/10.5101/nbe.v11i2.p157-169.
[13] Patra JK, Das G, Fraceto LF, et al. Nano based drug delivery systems: recent developments and future prospects. J Nanobiotechnol 2018;16(1). https://doi.org/10.1186/s12951-018-0392-8. PMid: 30231877.
[14] Peng Y, Chen L, Ye S, et al. Research and development of drug delivery systems based on drug transporter and nano-formulation. Asian J Pharm Sci 2020;15 (2):220–36. https://doi.org/10.1016/j.ajps.2020.02.004. PMid: 32373201.
[15] Al-Kinani MA, Haider AJ, Al-Musawi S. Design and synthesis of nanoencapsulation with a new formulation of Fe@Au-CS-CU-FA NPs by pulsed laser ablation in liquid (PLAL) method in breast cancer therapy: vitro and in vivo. Plasmonics 2021. https://doi.org/10.1007/s11468-021-01371-3.
[16] Dulińska-Litewka J, Łazarczyk A, Hałubiec P, et al. Superparamagnetic iron oxide nanoparticles-current and prospective medical applications. Materials (Basel) 2019;12(4):617. https://doi.org/10.3390/ma12040617. PMid: 30791358.
[17] Abdal Dayem A, Hossain M, Lee S, et al. The role of reactive oxygen species (ROS) in the biological activities of metallic nanoparticles. Int J Mol Sci 2017;18(1):120. https://doi.org/10.3390/ijms18010120. PMid: 28075405.
[18] Godeshala S, Nitiyanandan R, Thompson B, et al. Folate receptor-targeted aminoglycoside-derived polymers for transgene expression in cancer cells. Bioeng Transl Med 2016;1(2):220–31. https://doi.org/10.1002/btm2.10038. PMid: 29313013.
[19] Rezaei M, Hosseini SN, Khavari-Nejad RA, et al. HBs antigen and mannose loading on the surface of iron oxide nanoparticles in order to immuno-targeting: fabrication, characterization, cellular and humoral immunoassay. Artif Cells Nanomed Biotechnol 2019;47(1):1543–58. https://doi.org/10.1080/21691401.2019.1577888. PMid: 31007088.
[20] Mofazzal Jahromi MA, Al-Musawi S, Pirestani M, et al. Curcumin-loaded chitosan tripolyphosphate nanoparticles as a safe, natural and effective antibiotic inhibits the infection of *Staphylococcus aureus* and *Pseudomonas aeruginosa* in vivo. Iran J Biotech 2014;12(3):1–8. e1012.
[21] Ebadi M, Saifullah B, Buskaran K, et al. Synthesis and properties of magnetic nanotheranostics coated with polyethylene glycol/5-fluorouracil/layered double hydroxide. Int J Nanomed 2019;14:6661–78. https://doi.org/10.2147/IJN.S214923 PMid: 31695362.
[22] Yu S, Gao X, Baigude H, et al. Inorganic nanovehicle for potential targeted drug delivery to tumor cells, tumor optical imaging. ACS Appl Mater Interfaces 2015;7(9):5089–96. https://doi.org/10.1021/am507345j. PMid: 25693506.
[23] Eynali S, Khoei S, Khoee S, et al. Evaluation of the cytotoxic effects of hyperthermia and 5-fluorouracil-loaded magnetic nanoparticles on human colon cancer cell line HT-29. Int J Hyperth 2017;33(3):327–35. https://doi.org/10.1080/02656736.2016.1243260. PMid: 27701929.
[24] Watanabe M, Miyajima N, Igarashi M, et al. Sodium phenylacetate inhibits the Ras/MAPK signaling pathway to induce reduction of the c-Raf-1 protein in human and canine breast cancer cells. Breast Cancer Res Treat 2009;118 (2):281–91. https://doi.org/10.1007/s10549-008-0215-y. PMid: 18953652.
[25] Albukhaty S, Al-Musawi S, Abdul Mahdi S, et al. Investigation of dextran-coated superparamagnetic nanoparticles for targeted vinblastine controlled release, delivery, apoptosis induction, and gene expression in pancreatic cancer cells. Molecules 2020;25(20):. https://doi.org/10.3390/molecules25204721. PMid: 33076247E4721.
[26] Goodnough LH, DiNuoscio GJ, Ferguson JW, et al. Distinct requirements for cranial ectoderm and mesenchyme-derived Wnts in specification and differentiation of osteoblast and dermal progenitors. PLoS Genet 2014;10(2): e1004152. https://doi.org/10.1371/journal.pgen.1004152. PMid: 24586192.
[27] Al-Musawi S, Ibraheem S, Mahdi SA, et al. Smart nanoformulation based on polymeric magnetic nanoparticles and vincristine drug: a novel therapy for apoptotic gene expression in tumor. Life 2021;11(1):71. https://doi.org/10.3390/life11010071 PMid: 33478036.
[28] Al-Musawi S, Albukhaty S, Al-Karagoly H, et al. Dextran-coated superparamagnetic nanoparticles modified with folate for targeted drug delivery of camptothecin. Adv Nat Sci: Nanosci Nanotechnol 2020;11 (4):045009. https://doi.org/10.1088/2043-6254/abc75b.
[29] Naghibi Beidokhti HR, Ghaffarzadegan R, Mirzakhanlouei S, et al. Preparation, characterization, and optimization of folic acid-chitosan-methotrexate core-shell nanoparticles by box-behnken design for tumor-targeted drug delivery. AAPS PharmSciTech 2017;18(1):115–29. https://doi.org/10.1208/s12249-015-0445-3. PMid: 26896317.
[30] Al-Kaabi WJ, Albukhaty S, Al-Fartosy AJM, et al. Development of Inula graveolens (L.) plant extract electrospun/polycaprolactone nanofibers: a novel material for biomedical application. Appl Sci 2021;11(2):828. https://doi.org/10.3390/app11020828.
[31] Anirudhan TS, Christa J. Temperature and pH sensitive multi-functional magnetic nanocomposite for the controlled delivery of 5-fluorouracil, an anticancer drug. J Drug Delivery Sci Technol 2020;55:101476. https://doi.org/10.1016/j.jddst.2019.101476.
[32] Eftekhari A, Dizaj SM, Chodari L, et al. The promising future of nano-antioxidant therapy against environmental pollutants induced-toxicities. Biomed Pharmacother 2018;103:1018–27. https://doi.org/10.1016/j.biopha.2018.04.126. PMid: 29710659.
[33] Kaliyamoorthi K, Sumohan Pillai A, Alexander A, et al. Designed poly (ethylene glycol) conjugate-erbium-doped magnetic nanoparticle hybrid carrier: enhanced activity of anticancer drug. J Mater Sci 2021;56(5):3925–34. https://doi.org/10.1007/s10853-020-05466-w.
[34] Ahmadian E, Eftekhari A, Fard JK, et al. In vitro and in vivo evaluation of the mechanisms of citalopram-induced hepatotoxicity. Arch Pharm Res 2017;40 (11):1296–313. https://doi.org/10.1007/s12272-016-0766-0. PMid: 27271269.
[35] Ayyanaar S, Balachandran C, Bhaskar RC, et al. ROS-responsive chitosan coated magnetic iron oxide nanoparticles as potential vehicles for targeted drug delivery in cancer therapy. Int J Nanomed 2020;15:3333–46. https://doi.org/10.2147/IJN.S249240 PMid: 32494133.
[36] Xu R, Song P, Wang J, et al. Bioleaching of realgar nanoparticles using the extremophilic bacterium *Acidithiobacillus ferrooxidans* DLC. Electron J Biotechnol 2019;38:49–57. https://doi.org/10.1016/j.ejbt.2019.01.001.
[37] Pourali P, Badiee SH, Manafi S, et al. Biosynthesis of gold nanoparticles by two bacterial and fungal strains, *Bacillus cereus* and *Fusarium oxysporum*, and assessment and comparison of their nanotoxicity in vitro by direct and indirect assays. Electron J Biotechnol 2017;29:86–93. https://doi.org/10.1016/j.ejbt.2017.07.005.
[38] Ahmadi Nasab N, Hassani Kumleh H, Beygzadeh M, et al. Delivery of curcumin by a pH-responsive chitosan mesoporous silica nanoparticles for cancer treatment. Artif Cells Nanomed Biotechnol 2018;46(1):75–81. https://doi.org/10.1080/21691401.2017.1290648. PMid: 28278578.
[39] Marcucci F, Lefoulon F. Active targeting with particulate drug carriers in tumor therapy: fundamentals and recent progress. Drug Discov Today 2004;9 (5):219–28. https://doi.org/10.1016/S1359-6446(03)02988-X.
[40] Ma'mani L, Nikzad S, Kheiri-manjili H, et al. Curcumin-loaded guanidine functionalized PEGylated *I3ad* mesoporous silica nanoparticles KIT-6: practical strategy for the breast cancer therapy. Eur J Med Chem 2014;83:646–54. https://doi.org/10.1016/j.ejmech.2014.06.069. PMid: 25014638.
[41] Al-Musawi S, Albukhaty S, Al-Karagoly H, et al. Antibacterial activity of honey/chitosan nanofibers loaded with capsaicin and gold nanoparticles for wound dressing. Molecules 2020;25(20):4770. https://doi.org/10.3390/molecules25204770. PMid: 33080798.
[42] Moasser MM. The oncogene HER2: its signaling and transforming functions and its role in human cancer pathogenesis. Oncogene 2007;26(45):6469–87. https://doi.org/10.1038/sj.onc.1210477. PMid: 17471238.
[43] Dorard C, Estrada C, Barbotin C, et al. RAF proteins exert both specific and compensatory functions during tumour progression of NRAS-driven melanoma. Nat Commun 2017;8(1). https://doi.org/10.1038/ncomms15262. PMid: 28497782.
[44] Wang R, Geng N, Zhou Y, et al. Aberrant Wnt-1/beta-catenin signaling and WIF-1 deficiency are important events which promote tumor cell invasion and metastasis in salivary gland adenoid cystic carcinoma. Biomed Mater Eng

2015;26(1):S2145–53. https://doi.org/10.3233/BME-151520. PMid: 26405993.

[45] Hopwood B, Tsykin A, Findlay DM, et al. Gene expression profile of the bone microenvironment in human fragility fracture bone. Bone 2009;44(1):87–101. https://doi.org/10.1016/j.bone.2008.08.120. PMid: 18840552.

[46] Brücher BLDM, Keller G, Werner M, et al. Using Q-RT-PCR to measure cyclin D1, TS, TP, DPD, and Her-2/neu as predictors for response, survival, and recurrence in patients with esophageal squamous cell carcinoma following radiochemotherapy. Int J Colorectal Dis 2009;24(1):69–77. https://doi.org/10.1007/s00384-008-0562-5. PMid: 18704459.